Geosci. Model Dev. Discuss., 7, 1453–1476, 2014
www.geosci-model-dev-discuss.net/7/1453/2014/
doi:10.5194/gmdd-7-1453-2014

Geoscientific Model Development Discussions
Open Access

Numerical simulations of oceanic oxygen cycling in the FAMOUS Earth-System model: FAMOUS-ES, version 1.0

J. H. T. Williams[1], **I. J. Totterdell**[2], **P. R. Halloran**[3,*], **and P. J. Valdes**[1]

[1]BRIDGE, School of Geographical Sciences, University of Bristol, Bristol, BS8 1SS, UK
[2]Met Office Hadley Centre, FitzRoy Road, Exeter, EX1 3PB, UK
[3]School of Geography, University of Exeter, Exeter, EX4 4RJ, UK
[*]previously at: Met Office Hadley Centre, FitzRoy Road, Exeter, EX1 3PB, UK

Received: 9 January 2014 – Accepted: 10 February 2014 – Published: 21 February 2014

Correspondence to: J. H. T. Williams (jonny.williams@bristol.ac.uk)

Published by Copernicus Publications on behalf of the European Geosciences Union.

Abstract

Addition and validation of an oxygen cycle to the ocean component of the FAMOUS climate model are described. Surface validation is carried out with respect to HadGEM2-ES where good agreement is found and where discrepancies are mainly attributed to disagreement in surface temperature structure between the models. The agreement between the models at depth (where observations are also used in the comparison) in the Southern Hemisphere is less encouraging than in the Northern Hemisphere. This is attributed to a combination of excessive surface productivity in FAMOUS' equatorial waters (and its concomitant effect on remineralisation at depth) and its reduced overturning circulation compared to HadGEM2-ES. For the entire Atlantic basin FAMOUS has a circulation strength of 12.7 ± 0.4 Sv compared to 15.0 ± 0.9 for HadGEM2-ES. The HadGEM2-ES data used in this paper were obtained from the online database of the fifth Coupled Model Intercomparison Project, CMIP5 (Taylor et al., 2012).

1 Introduction

The ongoing model development of the FAMOUS climate model (Jones et al., 2005; Smith et al., 2008; Smith, 2012; Williams et al., 2013) in contrast to its higher resolution parent model HadCM3 (Gordon et al., 2000; Pope et al., 2000) is a testament to its utility as a fast (Fast Met Office UK Universities Simulator; FAMOUS) model which is capable of running at least 10 times faster than HadCM3. Model development with the latest Met Office Hadley Centre models continues apace however. Indeed huge improvements in model physics too numerous to detail here have been achieved via HadCM4 (Webb et al., 2001), HadGEM1 (e.g. Martin et al., 2006), HadGEM2 (e.g. Collins et al., 2011) and HadGEM3 (Hewitt et al., 2011); arguably the most notable of which are the introduction of a new semi-Lagrangian dynamical core in HadGEM1, and new ocean and cloud schemes in HadGEM3. It is not just the physical model components which have undergone model development however. HadCM3LC was

GMDD
7, 1453–1476, 2014

the first coupled climate model to include a fully interactive carbon cycle (Cox et al., 2000). HadGEM2-ES has extended the Earth System complexity represented within HadCM3LC by evolving the ocean carbon cycle sub-model, as well as the addition of a non-sulphate aerosols, aerosol indirect effects, interactive dust emission, and interactive tropospheric chemistry (Collins et al., 2011; Bellouin et al., 2011).

The continued use of the HadCM3 family of models is justified however since it has been shown to continue to perform well compared to other, more "up to date" models (Reichler and Kim, 2008; Nishii et al., 2012) and is capable of running for sufficiently long to allow slower components of the Earth system to be investigated.

There are many potential applications of the new model functionality presented here, for example the study of changes in oceanic oxygen content under climate change (Matear et al., 2000) and Cretaceous oceanic anoxic events, OAEs (e.g. Monteiro et al., 2012). These were episodes where potentially the entire global ocean was significantly depleted in oxygen, clearly with huge ramifications for global biogeochemical cycles. This paper however will focus solely on the model development undertaken to include cycling of oxygen in the FAMOUS model.

2 Theory

This work describes the inclusion of oxygen cycling into FAMOUS' ocean GCM code. The method followed is that of the second phase of the Ocean Carbon-Cycle Model Intercomparison Project, OCMIP2, as specifically implemented into the HadGEM2-ES code. The formalism used is that of Garcia and Gordon (1992) and full details of the biogeochemical cycling system present in FAMOUS (without oxygen) can be found in Palmer and Totterdell (2001). In the present work, the rate of biological production of oxygen is simply proportional to the rate of consumption of DIC (dissolved inorganic carbon),

$$\frac{\mathrm{d}O}{\mathrm{d}t} = -\alpha \frac{\mathrm{d}C}{\mathrm{d}t} \quad (1)$$

GMDD
7, 1453–1476, 2014

where O and C are the concentrations of oxygen and carbon (represented by dissolved inorganic carbon, DIC, in the model) and α is the constant of proportionality (equal to $\frac{138}{106}$). Although the continuity equations of oxygen and carbon dioxide are trivially similar, the form of the air–sea flux equations is quite different for oxygen. The form of the flux is as follows,

$$F_O = \rho k (1 - A)(O_{\text{sat}} - O). \quad (2)$$

In this equation, the flux, F_O is a function of the water density, ρ, the fractional coverage of sea ice (in each gridbox), A, the "piston velocity", k and the oxygen concentration at saturation point, O_{sat}. The functional forms of k and O_{sat} are now given,

$$k = 0.31 v^2 \sqrt{\frac{660}{S}} \quad (3)$$

$$O_{\text{sat}} = \frac{1000 e^A}{22.9316} \quad (4)$$

where v is the wind speed and S is the Schmidt number,

$$S = 1638 + T_c(-81.83 + T_c(1.483 - 0.008004 T_c)), \quad (5)$$

and A is given by

$$A = 2.00907 + 3.22014 T_s + 4.05010 T_s^2 + 4.94457 T_s^3 - 0.256847 T_s^4 + 3.88767 T_s^5 + H\left(-6.24523 \times 10^{-3} - 7.37614 \times 10^{-3} T_s + 1.03410 \times 10^{-2} T_s - 8.17083 \times 10^{-3} T_s^3\right) - 4.88682 \times 10^{-7} H^2. \quad (6)$$

In these equations, T_c and T_s are given by

$$T_c = \max(-2, \text{MIN}(40, T + 273.15)) \quad (7)$$

GMDD
7, 1453–1476, 2014

and

$$T_s = \ln\left(\left(\frac{5.713}{\mathrm{MAX}\left(2.71, 0.01\left(273.15+T\right)\right)}\right)-1\right). \quad (8)$$

and H is the salinity (strictly the halinity) in practical salinity units (PSU). Finally, the air–sea boundary condition is given by

$$\frac{\mathrm{d}O}{\mathrm{d}t} = \frac{F_O}{\Delta z_1}, \quad (9)$$

where Δz_1 is the depth of the first level in the ocean GCM vertical grid.

3 Validation

In the first documentation paper describing FAMOUS (Jones et al., 2005) the climatology was optimised such that it reproduced that of HadCM3 as accurately as possible. More recent incarnations of FAMOUS (e.g. Williams et al., 2013) have begun using observations and reanalyses as their targets however due to the model having largely outgrown its "simulator" label and becoming a fast-running Earth System Model in its own right.

Since the addition of an oxygen cycle to the ocean component of FAMOUS represents a completely new addition to the FAMOUS model (and HadCM3 family) it was deemed appropriate to compare the newly obtained climate model output to equivalent data from HadGEM2-ES, the main climate model used by the Met Office Hadley Centre in their submission to the Intergovernmental Panel Climate Change's fifth assessment report. This data is freely available online from the Programme for Climate Model Diagnosis and Intercomparison at http://pcmdi9.llnl.gov/esgf-web-fe/.

The horizontal resolution of the ocean GCM in HadGEM2-ES is 1° in the east–west plane. The same is true in the north–south plane but only between the poles and 30° from where the resolution increases to 0.33° on the equator. FAMOUS has a global

GMDD
7, 1453–1476, 2014

grid spacing of 2.5° × 3.75° and therefore has almost an order of magnitude reduction in areal resolution. HadGEM2-ES also has twice as many levels in the vertical (40) compared to FAMOUS (20). Figure 1 shows the predicted surface oxygen concentrations for FAMOUS and HadGEM2-ES as well as that observed by Helm et al. (2011). This observational dataset is used due to its recent use in validating the oxygen dynamics of HadGEM2-ES under climate change (Andrews et al., 2013).

In Fig. 1, the main areas of non-negligible disagreement occurring on the Antarctic coast, to the west of equatorial South America and northern mid-latitudes. In spite of these differences, the agreement between the two models is very encouraging, especially when the large disparity in overall model complexity and resolution is taken into account. The bottom right panel in Fig. 1 illustrates the scarcity of surface observations in the Helm et al. (2011) dataset and hence why the observations are not a useful benchmark for this latitude-longitude comparison.

Oxygen solubility is a strong negative function of temperature as it evident from Fig. 1 which shows (almost zonally symmetric) high values at the poles and lower values at the equator. It is therefore instructive to consider the sea surface temperature (SST) structure of the models and observations. This is shown in Fig. 2. The observational dataset is the 1870–1880 decadal mean from Rayner et al. (2003). This is the earliest decadal mean available and due to the age of this observational data, the spatial coverage is poor and is therefore heavily interpolated.

The most striking aspect of the temperature difference between FAMOUS and HadGEM2-ES in Fig. 2 is the consistent underestimation of Northern Hemisphere SSTs. This is in agreement with the previously noted (e.g. Williams et al., 2013) Northern Hemisphere cold bias in FAMOUS. Due to the negative correlation between temperature and oxygen solubility, it is expected that the surface oxygen concentration in this region in FAMOUS will be generally be higher than HadGEM2-ES and this is indeed seen in Fig. 1. Clearly there are other effects on surface oxygen concentration such as advection and diffusion of water masses and consumption and generation of oxygen through biogeochemical processes in the surface waters and these processes

GMDD
7, 1453–1476, 2014

are considered below. However the general pattern seen here is in line with first order thermodynamic expectations.

The statistical relationship between simulated and observed surface oxygen concentrations is studied by sampling only the data points in Fig. 1 where observational data are present. These plots are shown in Fig. 3.

From Fig. 3 it is clear that FAMOUS generally overestimates the observed values. The average value of this difference is $14.5 \pm 25.5\,\mu mol\,L^{-1}$ where the error estimate is 1 standard deviation (σ). The equivalent value for HadGEM2-ES vs. observations is $8.3 \pm 17.7\,\mu mol\,L^{-1}$ and therefore HadGEM2-ES not only gives a closer fit to the observed values but a more consistently varying one (i.e. lower standard deviation). The comparison of FAMOUS and HadGEM2-ES gives a value of $6.2 \pm 28.1\,\mu mol\,L^{-1}$ (FAMOUS greater than HadGEM2-ES).

Figure 2 shows that there are some regions where the models' representation of SST differ significantly and so it is of interest to consider only areas where the models are in relative agreement. To this end the data have been further sub-sampled to include only areas where the models disagree by 2 °C or less. The value for the comparison between FAMOUS and observations is now $9.9 \pm 24.7\,\mu mol\,L^{-1}$, i.e. a decrease of 32 % in the average difference but only a marginal decrease in the variability. The results for HadGEM2-ES compared to observations are now $8.2 \pm 17.4\,\mu mol\,L^{-1}$ which are virtually unchanged with respect to previous results.

The improved agreement between FAMOUS and observations in these sub-sampled data simply shows that when FAMOUS agrees with HadGEM2-ES, it also agrees better with observations. This is simply a reflection of the better agreement of HadGEM2-ES with observations in the first place. The essentially unchanged results in the HadGEM2-ES comparison with observations are further proof of this fact, i.e., the points which are discarded in this secondary analysis represent points which are indicative of FAMOUS' lack of agreement with observations. Whilst this analysis does give results which are intuitively correct, the highly sparse nature of oxygen observations (Fig. 1) makes this analysis of model agreement with observations virtually impossible "by eye". The same

GMDD
7, 1453–1476, 2014

point holds for the SST data (which is also sparse for this time period, as mentioned above) although it is presented in an interpolated format in the Rayner at al. (2003) dataset.

Figure 4 shows the comparison in a zonal mean-depth sense where the observations can provide a useful target for validation. The observed oxygen data in Fig. 4 has a vertical resolution of 50 m throughout the water column.

Firstly considering the agreement between the models, it is clear that, qualitatively, the oxygen structure of FAMOUS is in good agreement with HadGEM2-ES although the oxygen maxima at high northern latitudes are somewhat underestimated in FAMOUS.

The main area of disagreement in Fig. 4 – both between the models and between the respective models and the observations – is at depth in the Southern Hemisphere where FAMOUS significantly underestimates the oxygen concentration.

To examine this issue further, it is necessary to consider both the continuity (i.e. oxygen "amount") of sinking organic matter in the model as well as the ocean overturning because this will ultimately affect whether or not surface oxygen will be transported to depth. Both of these effects are now considered in turn. Equation (10) is from Palmer and Totterdell (2001) and gives the concentration of detritus as a function of time.

$$\left.\frac{\partial D}{\partial t}\right|_{\text{biology}} = m_D P^2 + \frac{1}{3}\left(\mu_1 Z + \mu_2 Z^2\right) + E_D - \lambda D - G_\text{d}, \tag{10}$$

where

$$m_D = m \cdot \min\left(1, \frac{C_\text{p}}{C_\text{d}}\right) \tag{11}$$

and

$$E_D = \min\left(\left(G_\text{p} + G_\text{d} - G_\text{z}\right), \frac{\left(C_\text{p}G_\text{p} + C_\text{d}G_\text{d} - C_\text{z}G_\text{z}\right)}{C_\text{d}}\right). \tag{12}$$

GMDD
7, 1453–1476, 2014

In these preceding three equations, D, P and Z are the detritus, phytoplankton and zooplankton concentrations, m_D is the phytoplankton mortality rate constant, $\mu_{1,2}$ are the constant and zooplankton-dependent mortality coefficients, E_D is the rate of detritus formation due to egestion, λ is the (depth dependent) remineralisation rate, G_z is the zooplankton grazing rate, $C_{p,z,d}$ are the carbon : nitrogen ratios in phytoplankton, zooplankton and detritus and $G_{d,p}$ are the grazing rates of zooplankton on detritus and phytoplankton respectively. Finally,

$$m = \begin{cases} 0, & P \leq 0.01\,\mu\text{mol}\,\text{L}^{-1}, \\ m_0, & \text{otherwise}, \end{cases} \tag{13}$$

where m_0 is the mortality rate of phytoplankton.

Figure 5 shows the surface net primary productivity (NPP) for FAMOUS and HadGEM2-ES compared to available observations (Behrenfeld and Falkowski, 1997).

Figure 5 clearly shows that both models overestimate equatorial NPP. This overestimation is largest in the Pacific and is significantly larger in FAMOUS. This behaviour has been noted previously in Williams et al. (2013) where the current setup of FAMOUS was compared to previous incarnations. This spike in productivity will lead to an increased amount of detritus sinking out of the photic zone (top few hundred metres) of the ocean which will then undergo remineralisation. This is qualitatively the reverse of photosynthesis and therefore consumes oxygen, hence reducing the oxygen content.

As stated above, the amount of oxygen produced and consumed is one factor in a dynamic system's behaviour, but for a full understanding, the transport must also be considered. Equation 14 shows the three dimensional continuity equation for a generic density ρ and velocity vector field $\boldsymbol{u}$.

$$\frac{\partial \rho}{\partial t} + \nabla \cdot (\rho \boldsymbol{u}) + G_{\text{O}}^{+} - G_{\text{O}}^{-} = 0, \tag{14}$$

where G_{O}^{+} and G_{O}^{-} represent generation and consumption of oxygen due to, for example, photosynthesis and remineralisation. Figures 6 and 7 show the meridional

GMDD
7, 1453–1476, 2014

overturning circulation (MOC) in Sverdrups (millions of cubic metres per second) for FAMOUS and HadGEM2-ES in the global and Atlantic oceans respectively (note the different latitude limits in the two figures). The ocean basins themselves are shown in Fig. 8.

Qualitatively, the agreement between the circulation patterns in Fig. 6 is encouraging although it is clear that FAMOUS significantly underestimates the circulation seen in HadGEM2-ES. Assuming that this circulation has an important effect on the oxygen concentration through reduced ventilation, the significantly reduced Southern Hemisphere circulation in FAMOUS compared to HadGEM2-ES should result in a large decrease in the oxygen concentration in this region, which is indeed seen in Fig. 4.

From a more quantitative angle, the overturning on the basin scale is now interrogated. Kanzow et al. (2010) have given an observed value of 18.7 ± 2.7 Sv for the maximum absolute value of the Atlantic basin overturning at 26.5° N. For the four HadGEM2-ES realisations studied here (the results presented above are the ensemble mean) a value of 12.7 ± 0.6 Sv is found and for FAMOUS, 12.7 ± 0.4 Sv. The uncertainty estimate in FAMOUS is obtained by calculating the overturning for last four 30 yr periods of a 3500 yr run. These figures are in agreement with previously published data on HadGEM2-ES from Martin et al., 2011, (13.3 ± 1.0 Sv at 26° N for a pre-industrial simulation) but are weaker than the 2004–2008 estimate of Kanzow et al. (2010) given above and the HadGEM2-ES figures for the period 1990–2000 (16.0 ± 1.0 Sv at 30° N) from Martin et al. (2011).

Figure 7 shows that HadGEM2-ES has well developed upper and lower circulatory cells which are analogous to the (upper) North Atlantic Deep Water (NADW) and (lower) Antarctic Bottom Water (AABW) systems observed in Talley et al. (2003). This AABW water cell in the Atlantic basin is not present in FAMOUS. This shows that Southern Hemisphere water is not being circulated into northern latitudes and hence that the general circulation in this region is more sluggish than HadGEM2-ES and adds further evidence that the circulation in FAMOUS is being underestimated compared to HadGEM2-ES.

GMDD
7, 1453–1476, 2014

Now taking the Atlantic basin as a whole, the study of Talley et al. (2003) is used and the numerical information is given in Table 1 along with the data for 26.5° N given above (note that Fig. 7 gives the maximum Atlantic overturning value for FAMOUS at approximately 26° N). The lower value for FAMOUS compared to HadGEM2-ES is in agreement with the results noted above, i.e. that the circulation in FAMOUS is generally more sluggish than HadGEM2-ES. The fact that both models underestimate the value of 18 Sv given by Talley et al. however should be tempered by the fact that the the authors give an error estimate of between 3 and 5 Sv on their circulation magnitudes.

4 Conclusions

This paper describes an update to the latest version of FAMOUS (Williams et al., 2013) in which a numerically calculated oxygen cycle is included for the first time. This follows the scheme of the latest Hadley Centre GCM, HadGEM2-ES, under the auspices of the second phase of the Ocean Carbon-Cycle Model Intercomparison Project, OCMIP2. The surface oxygen concentration is in good agreement with that of HadGEM2-ES. FAMOUS' general overestimation of the Northern Hemisphere surface oxygen concentration is attributed to its underestimation of SST. When the model output is compared against available surface observations on a point-by-point basis, both models generally overestimate the observed values although this overestimation is reduced in HadGEM2-ES.

The agreement between the simulated oxygen concentrations at depth in the Northern Hemisphere is also encouraging. The deep Southern Hemisphere agreement is less good however. This is partially ascribed to FAMOUS' overestimation of equatorial net primary productivity which causes increased remineralisation of sinking detritus at depth and hence increased oxygen consumption. This is further exacerbated by reduced ocean circulation in FAMOUS compared to HadGEM2-ES which acts to reduce Southern Hemisphere ventilation. This reduction in circulatory strength is evident in both the global and Atlantic oceans.

GMDD
7, 1453–1476, 2014

Finally, the authors feel that with recent developments in the terrestrial and oceanic carbon cycles and now with the introduction of oceanic oxygen, the FAMOUS model is leaving the traditional "climate model" definition and moving into the realm of an "Earth-System model", hence the title of this paper.

5 Code availability

The main repository for the Met Office Unified Model (UM) at the version corresponding to the model presented here can be found at http://cms.ncas.ac.uk/code_browsers/UM4.5/UMbrowser/index.html.

6 Supplement

The code detailing the advances described in this paper is completely contained within one text file (known as a code modification file or "mod") and this is available as supplementary material to this paper. This is protected under Crown Copyright, as is the base code linked above.

Supplementary material related to this article is available online at http://www.geosci-model-dev-discuss.net/7/1453/2014/gmdd-7-1453-2014-supplement.zip.

Acknowledgement. J. H. T. Williams and P. J. Valdes were supported by funding from Statoil ASA, Norway. J. H. T. Williams and P. J. Valdes thank T. L. Leith of Statoil ASA for extensive discussions throughout this work. I. J. Totterdell and P. R. Halloran were supported by the Joint DECC/Defra Met Office Hadley Centre Climate Programme (GA01101).

References

Andrews, O. D., Bindoff, N. L., Halloran, P. R., Ilyina, T., and Le Quéré, C.: Detecting an external influence on recent changes in oceanic oxygen using an optimal fingerprinting method, Biogeosciences, 10, 1799–1813, doi:10.5194/bg-10-1799-2013, 2013.

Behrenfeld, M. J. and Falkowski, P. G.: Photosynthetic rates derived from satellite-based chlorophyll concentration, Limnol. Oceanogr., 42, 1–20, 1997.

Bellouin, N., Rae, J., Jones, A., Johnson, C., Haywood, J., and Boucher, O.: Aerosol forcing in the climate model intercomparison project (CMIP5) simulations by HadGEM2-ES and the role of ammonium nitrate, J. Geophys. Res., 116, D20206, doi:10.1029/2011JD016074, 2011.

Collins, W. J., Bellouin, N., Doutriaux-Boucher, M., Gedney, N., Halloran, P., Hinton, T., Hughes, J., Jones, C. D., Joshi, M., Liddicoat, S., Martin, G., O'Connor, F., Rae, J., Senior, C., Sitch, S., Totterdell, I., Wiltshire, A., and Woodward, S.: Development and evaluation of an Earth-System model – HadGEM2, Geosci. Model Dev., 4, 1051–1075, doi:10.5194/gmd-4-1051-2011, 2011.

Cox, P. M., Betts, R. A., Jones, C. D., Spall, S., A., and Totterdell, I. J.: Acceleration of global warming due to carbon-cycle feedbacks in a coupled climate model, Nature, 408, 184–187, 2000.

Garcia, H. E. and Gordon, L. I.: Oxygen solubility in seawater: better fitting equations, Limnol. Oceanogr., 37, 1307–1312, 1992.

Gordon, C., Cooper, C., Senior, C. A., Banks, H., Gregory, J. M., Johns, T. C., Mitchell, J. F. B., and Wood, R. A.: The simulation of SST, sea ice extents and ocean heat transports in a version of the Hadley Centre coupled model without flux adjustments, Clim. Dynam., 16, 147–168, 2000.

The HadGEM2 Development Team: G. M. Martin, Bellouin, N., Collins, W. J., Culverwell, I. D., Halloran, P. R., Hardiman, S. C., Hinton, T. J., Jones, C. D., McDonald, R. E., McLaren, A. J., O'Connor, F. M., Roberts, M. J., Rodriguez, J. M., Woodward, S., Best, M. J., Brooks, M. E., Brown, A. R., Butchart, N., Dearden, C., Derbyshire, S. H., Dharssi, I., Doutriaux-Boucher, M., Edwards, J. M., Falloon, P. D., Gedney, N., Gray, L. J., Hewitt, H. T., Hobson, M., Huddleston, M. R., Hughes, J., Ineson, S., Ingram, W. J., James, P. M., Johns, T. C., Johnson, C. E., Jones, A., Jones, C. P., Joshi, M. M., Keen, A. B., Liddicoat, S., Lock, A. P., Maidens, A. V., Manners, J. C., Milton, S. F., Rae, J. G. L., Ridley, J. K., Sellar, A.,

GMDD
7, 1453–1476, 2014

Senior, C. A., Totterdell, I. J., Verhoef, A., Vidale, P. L., and Wiltshire, A.: The HadGEM2 family of Met Office Unified Model climate configurations, Geosci. Model Dev., 4, 723–757, doi:10.5194/gmd-4-723-2011, 2011.

Helm, K. P., Bindoff, N. L., and Chrusch, J. A.: Observed decreases in oxygen content of the global ocean, Geophys. Res. Lett., 38, L23602, doi:10.1029/2011GL049513, 2011.

Hewitt, H. T., Copsey, D., Culverwell, I. D., Harris, C. M., Hill, R. S. R., Keen, A. B., McLaren, A. J., and Hunke, E. C.: Design and implementation of the infrastructure of HadGEM3: the next-generation Met Office climate modelling system, Geosci. Model Dev., 4, 223–253, doi:10.5194/gmd-4-223-2011, 2011.

Jones, C., Gregory, J., Thorpe, R., Cox, P., Murphy, J., Sexton, D., and Valdes, P.: Systematic optimisation and climate simulations of FAMOUS, a fast version of HadCM3, Clim. Dynam., 25, 189–204, 2005.

Kanzow, T., Cunningham, S. A., Johns, W. E., Hirschi, J. J.-M., Marotzke, J., Baringer, M. O., Meinen, C. S., Chidichimo, M. P., Atkinson, C., Beal, L. M., Bryden, H. L., and Collins, J.: Seasonal variability of the Atlantic meridional overturning circulation at 26.5° N, J. Climate, 23, 5678–5698, 2010.

Martin, G. M., Ringer, M. A., Pope, V. D., Jones, A., Dearden, C., and Hinton, T. J.: The physical properties of the atmosphere in the new Hadley Centre Global Environmental Model (HadGEM1) – Part 1: Model description and global climatology, J. Climate, 19, 1274–1301, 2006.

Matear, R. J., Hirst, A. C., and McNeil, B. I.: Changes in dissolved oxygen in the Southern Ocean with climate change, Geochem. Geophy. Geosy., 1, 2000GC000086, doi:10.1029/2000GC000086, 2000.

Monteiro, F. M., Pancost, R. D., Ridgwell, A., and Donnadieu, Y.: Nutrients as the dominant control on the spread of anoxia and euxinia across the Cenomanian-Turonian ocean anoxic event (OAE2): model-data comparison, Paleoceanography, 27, PA4209, doi:10.1029/2012PA002351, 2012.

Nishii, K., Miyasaka, T., Nakamura, H., Kosaka, Y., Yokoi, S., Takayabu, Y. N., Endo, H., Ichikawa, H., Oshima, K., Sato, N., and Tsushima, Y.: Relationship of the reproducibility of multiple variables among global climate models, J. Meteorol. Soc. Jpn., 90A, 87–100, doi:10.2151/jmsj.2012-A04, 2012.

Palmer, J. R. and Totterdell, I. J.: Production and export in a global ocean ecosystem model, Deep-Sea Res. Pt. I, 48, 1169–1198, 2001.

GMDD
7, 1453–1476, 2014

Pope, V. D., Gallani, M. L., Rowntree, P. R., and Stratton, R. A.: The impact of new physical parametrizations in the Hadley Centre climate model: HadAM3, Clim. Dynam., 16, 123–146, 2000.

Rayner, N. A., Parker, D. E., Horton, E. B., Folland, C. K., Alexander, L. V., Rowell, D. P., Kent, E. C., and Kaplan, A.: Global analyses of sea surface temperature, sea ice, and night marine air temperature since the late nineteenth century, J. Geophys. Res., 108, 4407, doi:10.1029/2002JD002670, 2003.

Reichler, T. and Kim, J.: How well do coupled models simulate today's climate?, B. Am. Meteorol. Soc., 89, 303–311, doi:10.1175/BAMS-89-3-303, 2008.

Smith, R. S.: The FAMOUS climate model (versions XFXWB and XFHCC): description update to version XDBUA, Geosci. Model Dev., 5, 269–276, doi:10.5194/gmd-5-269-2012, 2012.

Smith, R. S., Gregory, J. M., and Osprey, A.: A description of the FAMOUS (version XDBUA) climate model and control run, Geosci. Model Dev., 1, 53–68, doi:10.5194/gmd-1-53-2008, 2008.

Talley, L. D., Reid, J. L., and Robbins, P. E.: Data-based meridional overturning streamfunctions for the global ocean, J. Climate, 16, 3213–3226, 2003.

Taylor, K. E., Stouffer, R. J., and Meehl, G. A.: An overview of CMIP5 and the experiment design, B. Am. Meteorol. Soc., 93, 485–498, doi:10.1175/BAMS-D-11-00094.1, 2012.

Webb, M., Senior, C., Bony, S., and Morcrette, J-J: Combining ERBE and ISCCP data to assess clouds in the Hadley Centre, ECMWF and LMD atmospheric climate models, Clim. Dynam., 17, 905–922, 2001.

Williams, J. H. T., Smith, R. S., Valdes, P. J., Booth, B. B. B., and Osprey, A.: Optimising the FAMOUS climate model: inclusion of global carbon cycling, Geosci. Model Dev., 6, 141–160, doi:10.5194/gmd-6-141-2013, 2013.

GMDD
7, 1453–1476, 2014

Table 1. Atlantic meridional overturning circulation (MOC) in Sv. Note the lack of an error estimate for the Talley et al. figures. The authors of this paper note "Uncertainty in the diagnosed streamfunction is large, on the order of 3–5 Sv".

	FAMOUS	HadGEM2-ES	Kanzow et al. (2010)	Talley et al. (2003)
Atlantic (26.5° N)	12.7 ± 0.4	12.7 ± 0.6	18.7 ± 2.7	–
Atlantic	12.7 ± 0.4	15.0 ± 0.9	–	18

GMDD
7, 1453–1476, 2014

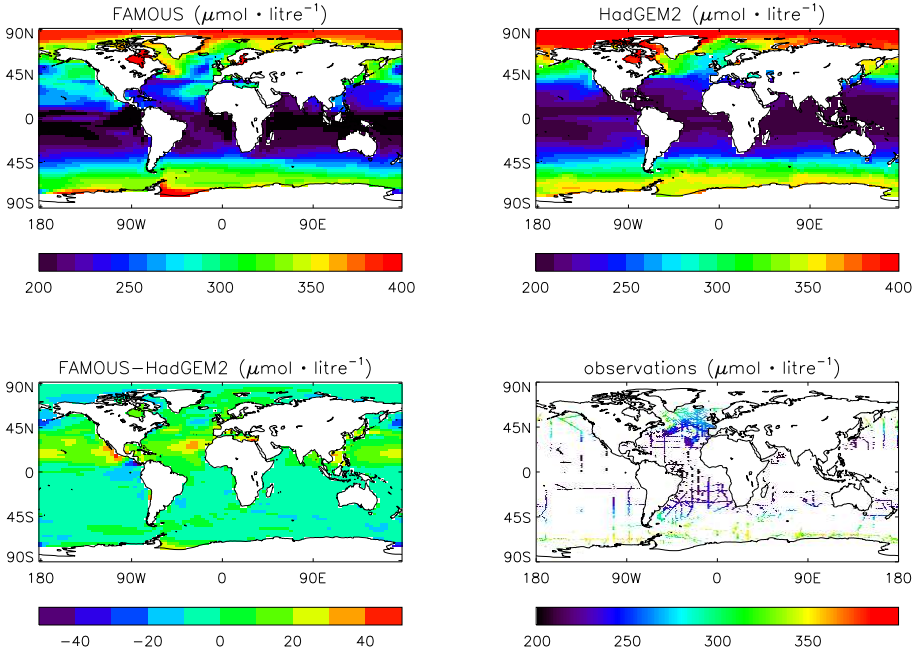

Fig. 1. Surface oxygen concentrations (μmol kg^{-1}) for FAMOUS (top left) and HadGEM2-ES (top right). The percentage difference between the two is shown in the bottom left panel and the paucity of observations (Helm et al., 2011) is illustrated in the bottom right panel.

GMDD
7, 1453–1476, 2014

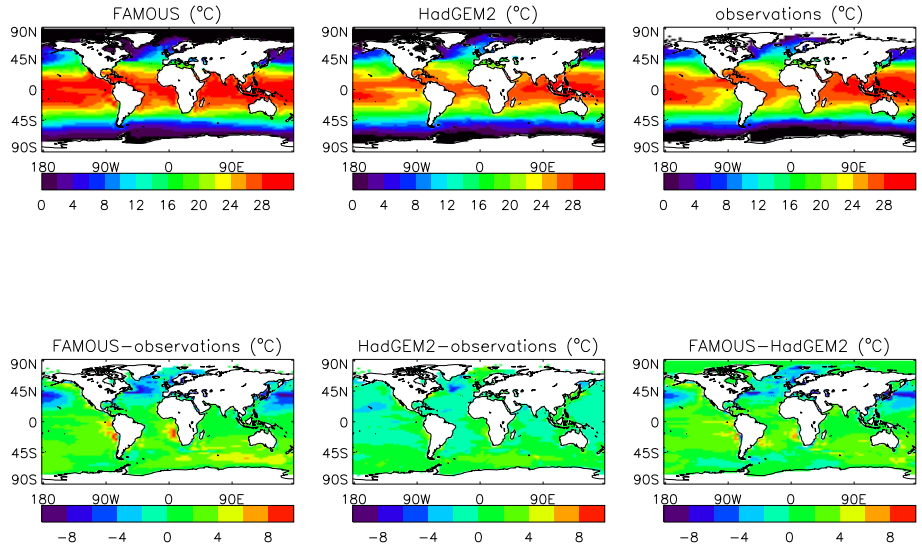

Fig. 2. SSTs for FAMOUS (top left), HadGEM2-ES (top middle) and observations (top right). Difference plots between the models and observations are shown in the bottom left and middle left panels and the difference between the models themselves is shown in the bottom right.

GMDD
7, 1453–1476, 2014

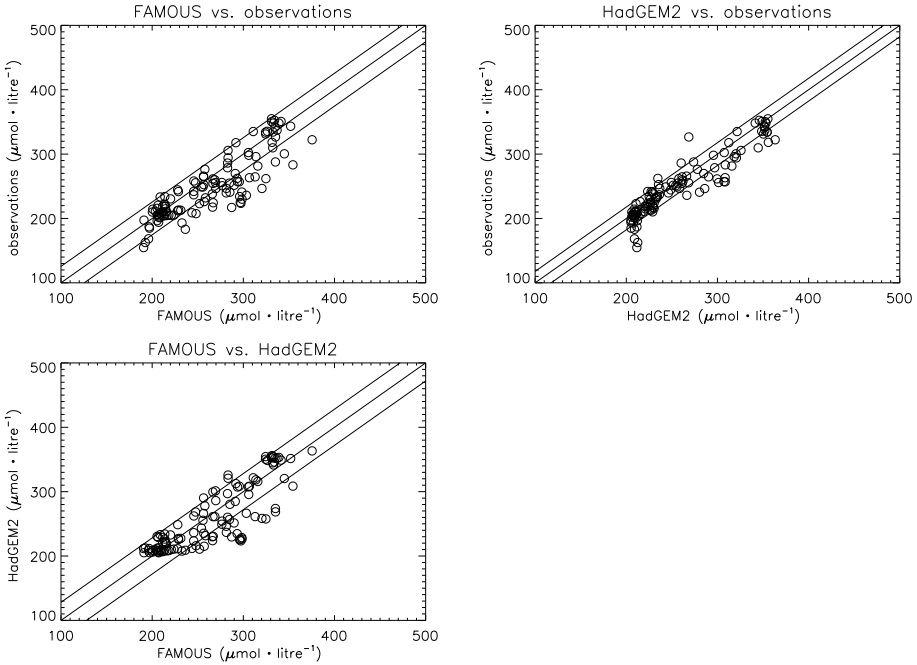

Fig. 3. Scatter plots showing the relationships between simulated and observed surface oxygen concentrations. Data have been sampled so that only data points where observational data are available are shown (Fig. 1, bottom right). The three lines show the 1 : 1 line and ±1 standard deviation (1σ) of the difference between the two quantities.

GMDD
7, 1453–1476, 2014

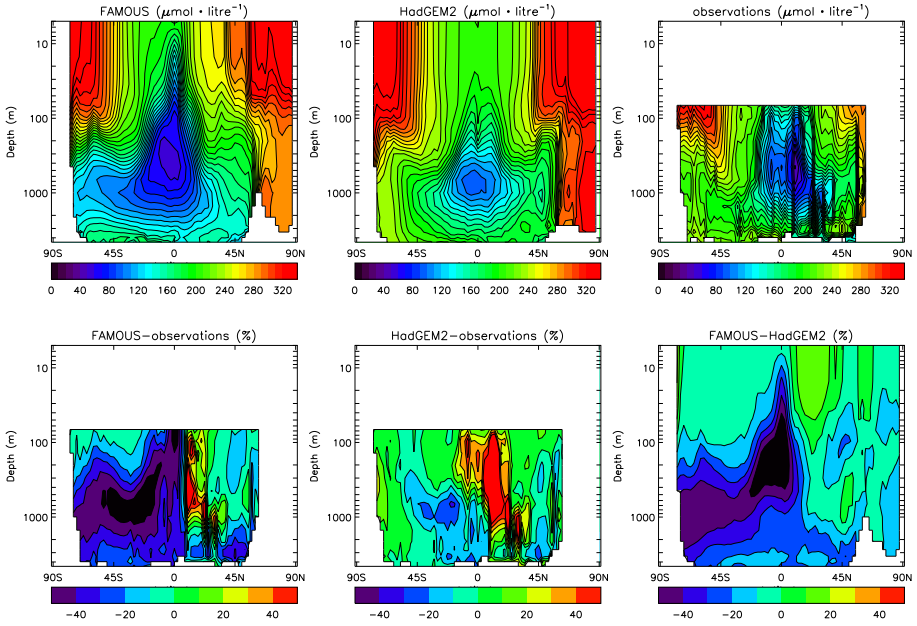

Fig. 4. Zonal mean-depth oxygen concentrations (μmol L^{-1}) for FAMOUS (top left), HadGEM2-ES (top middle) and observations (top right). Percentage difference plots between the models and observations are shown in the bottom left and middle left panels and the difference between the models themselves is shown in the bottom right.

GMDD
7, 1453–1476, 2014

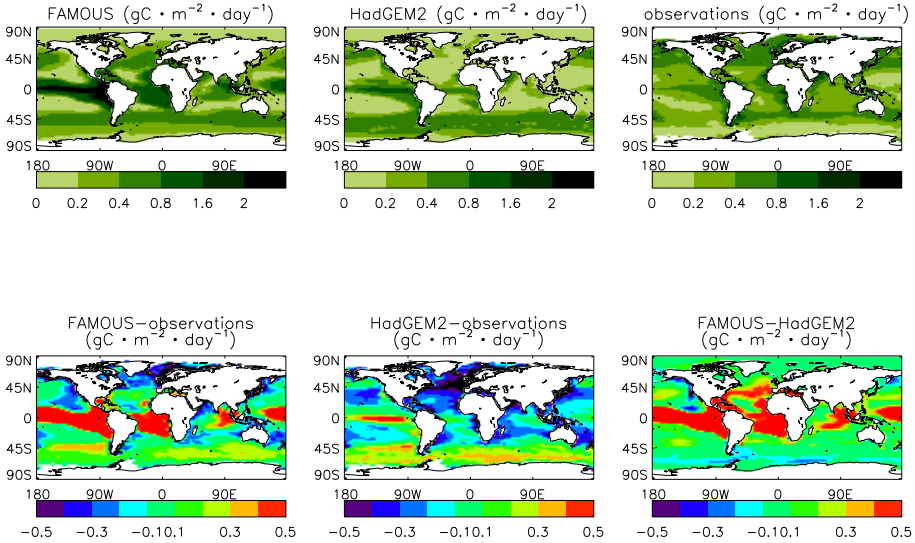

Fig. 5. Net primary productivity (NPP) (gC m^{-2} day^{-1}) for FAMOUS (top left), HadGEM2-ES (top middle) and observations (top right). Absolute difference plots between the models and observations are shown in the bottom left and middle left panels and the difference between the models themselves is shown in the bottom right.

GMDD
7, 1453–1476, 2014

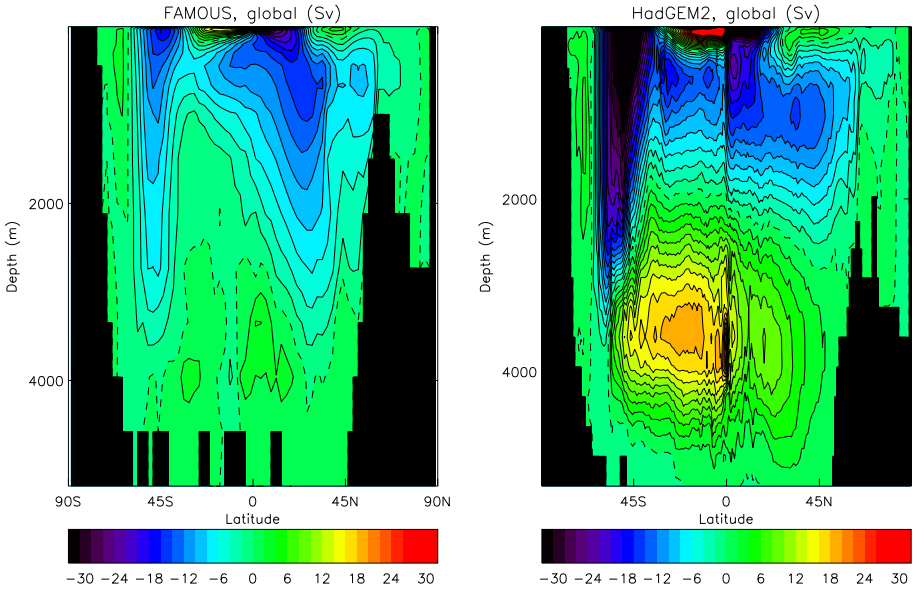

Fig. 6. Global meridional overturning circulation (MOC) in FAMOUS (left) and HadGEM2-ES (right). The zero contour is dashed.

GMDD
7, 1453–1476, 2014

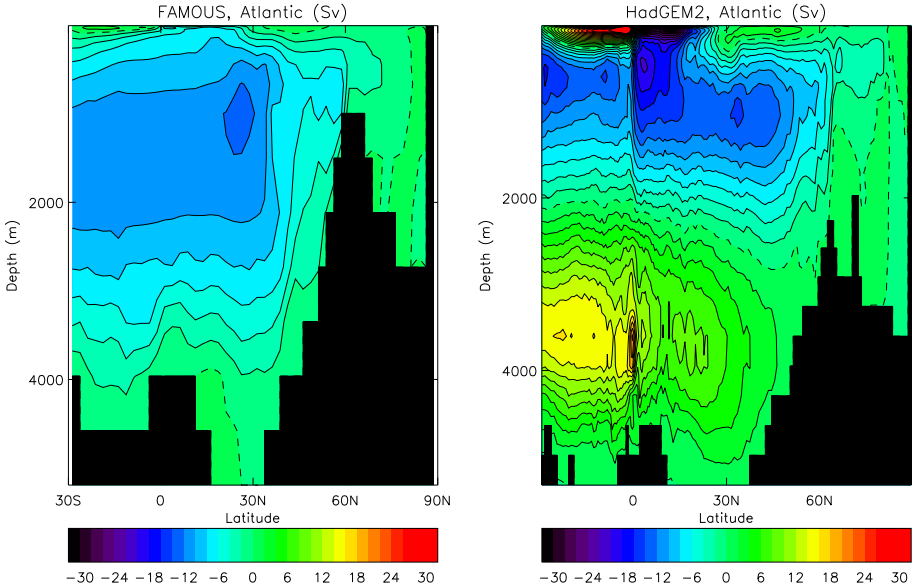

Fig. 7. Atlantic meridional overturning circulation (MOC) in FAMOUS (left) and HadGEM2-ES (right). The zero contour is dashed.

GMDD
7, 1453–1476, 2014

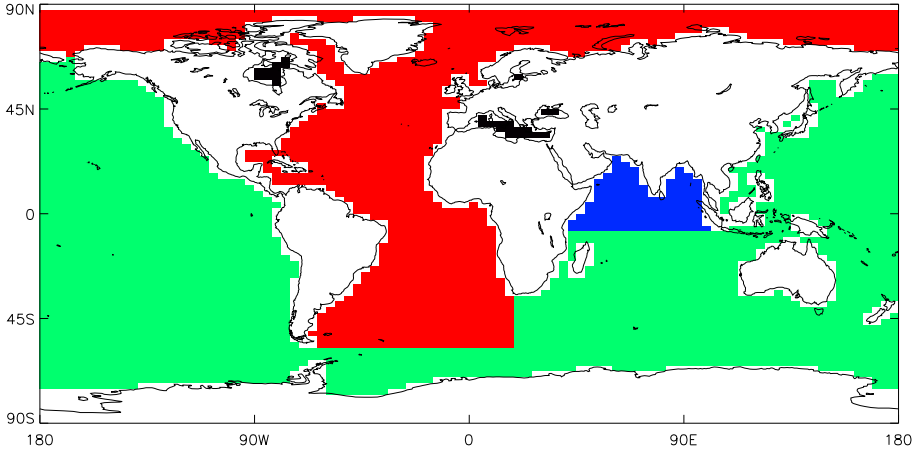

Fig. 8. The breakdown of ocean basins in meridional overturning circulation calculations. Note that enclosed basins such as the Mediterranean Sea are excluded from these calculations and are coloured black. The Atlantic is red, the Pacific green and the Indian Ocean blue.

GMDD
7, 1453–1476, 2014